Transitional flow of a yield stress fluid in a pipe: Evidence of a robust coherent structure

Ahmed Esmael, Chérif Nouar

Transitional flow of a yield stress fluid in a pipe: Evidence of a robust coherent structure

A. Esmael and C. Nouar
LEMTA UMR 7563 CNRS - Nancy Université
2 Avenue de la Foret de Haye,
BP 160, 54504 Vandoeuvre, France
(Dated: November 7, 2007)

In two independent articles, Escudier and Presti [1] and Peixinho *et al.* [2] studied experimentally the flow structure of a yield stress fluid in a cylindrical pipe. It was observed that the mean velocity profiles were axisymmetric in the laminar and turbulent regimes, and presented an increasing asymmetry with increasing Reynolds number in the transitional regime. The present paper provides a three-dimensional description of this asymmetry from axial velocity profiles measurements at three axial positions and different azimuthal positions. The observed transitional flow suggests the existence of a robust non-linear coherent state characterized by two weakly modulated counter-rotating longitudinal vortices. This new state mediates the transition between laminar and turbulent flow and is qualitatively similar to the *edge-states* recently computed in the newtonian case [3–5].

PACS numbers: 47.27.nf,47.50-d,47.20.-k

Introduction. Understanding the mechanism of transition from laminar to turbulent flow of Newtonian fluids has been an ongoing quest for more than a century. It is only during this last decade that considerable advances have been made with the discovery of new numerical solutions which make it possible to clear the deadlock in which the studies of transition of linearly stable flows were. For Newtonian fluid flow in a pipe of circular cross section, based on the self-sustained-process (SSP) theory developed by Waleffe [6] and the subsequent nonlinear continuation approach [7], a family of three-dimensional travelling waves which propagate at a constant phase speed in the streamwise direction were discovered by Faisst and Eckhard [8] and Wedin and Kerswell [9]. These travelling waves (TW) originate in saddle-node bifurcations and are immediately linearly unstable. They are dominated by pairs of downstream vortices and streaks and are very similar to the coherent structures observed experimentally in equilibrium puffs [10]. TW's of 1-fold through 6-fold symmetries have been found, but only 2,3- and 4-fold TW's are currently known to exist below a Reynolds number $Re = (\rho U_B D)/\mu = 2485$, where ρ is the fluid density, U_B the bulk velocity and $D = 2R$ is the pipe diameter. Very recently asymmetric TW composed by two rolls in the cross-section have been computed [3–5]

Concerning transition to turbulence for non Newtonian fluids flows, very little is available in the literature, despite the importance of this problem in the design and control of several industrial processes such as in oil-well cementing, extrusion of molten polymers, paper coating, etc. Nevertheless, the existing literature reveals an interesting and yet unexplained effect: Above a certain Reynolds number the mean flow develops a stable asymmetry, while in the laminar and turbulent regimes the flow is axisymmetric. Independent observations of this asymmetry have been made by Escudier and Presti [1] and Peixinho *et al.* [2]. These two groups have recently jointly published these, and additional observations in [11] to highlight the effect. It was also clearly indicated in [11] that this asymmetry is not a consequence of the Coriolis force arising from the earth rotation. Likewise, the temperature gradients as well as the longitudinal curvature of the pipe are too weak to modify the velocity profile. Therefore, the asymmetry of the velocity profiles observed in [1] and [2] is a consequence of a fluid-dynamical mechanism rather than an experimental artifact. This conclusion is supported by two different studies: (i) an experimental study of Eliahou *et al.* [12] on the transitional pipe flow for Newtonian fluid and (ii) direct numerical simulation of the weakly turbulent pipe flow of shear thinning fluid performed by Rudman *et al.* [13]. In the first study, an asymmetric distortion of the mean velocity profiles is observed only when a high amplitude asymmetric perturbation is imposed. In the second one, the authors indicate that for sufficiently shear thinning behavior (power-law fluid with $n = 0.5$), "the active region of the flow continually moves along the pipe and appears to preferentially occur at one azimuthal location for extended times."

The aim of the present paper is to provide a three-dimensional description of the asymmetry. A non-linear robust coherent state will be highlighted and its contribution to structuring the transition process will be discussed. As a starting point, we consider the linear stability of Hagen-Poiseuille flow of a yield stress fluid.

Linear theory. First of all, we recall that the one-dimensional shear flow of a yield stress fluid is mainly characterized by the presence of a plug zone of radius r_0 moving as a rigid body. In the sheared zone, between the wall at $r = R$ and the yield surface at $r = r_0$, the effective viscosity μ decreases non-linearly with increasing shear rate. Actually, μ is infinite at the yield surface and decreases when approaching the wall. In the following, it is assumed that the rheological behavior of the fluid can be described by the Herschel-Bulkley model. For unidi-

rectional shear flow with velocity U_ℓ in the z direction, the relationship between the shear stress τ_{rz} and the velocity gradient dU_ℓ/dr is:

$$\tau_{rz} = sgn(dU_\ell/dr)\tau_0 + K\left|\frac{dU_\ell}{dr}\right|^{n-1}\frac{dU_\ell}{dr} \;\Leftrightarrow\; |\tau_{rz}| \geq \tau_0,$$
$$dU_\ell/dr = 0 \;\Leftrightarrow\; |\tau_{rz}| \leq \tau_0,$$

where τ_0 is the yield stress, n the flow behavior index and K is the consistency index. The axial velocity profile $U_\ell(r)$ is given by

$$\frac{U_\ell(r)}{U_B} = \begin{cases} \frac{U_{\ell max}}{U_B} & ;\ 0 \leq r \leq r_0, \\ \frac{U_{\ell max}}{U_B}\left[1 - \left(\frac{r-r_0}{R-r_0}\right)^{\frac{n+1}{n}}\right] & ;\ r_0 \leq r \leq R, \end{cases} \quad (1)$$

with

$$\frac{U_{\ell max}}{U_B} = \frac{n}{n+1}\left(\frac{Hb}{a}\right)^{1/n}(1-a)^{\frac{n+1}{n}},$$

where U_B is the bulk velocity, $a = r_0/R$ and $Hb = \frac{\tau_0 R^n}{K {U_B}^n}$ is the Herschel-Bulkley number. The base flow is governed by two parameters n and a or n and Hb. The dependence of a with respect to n and Hb can be found using the continuity equation in integral form [2].

The linear stability of Hagen-Poiseuille flow of Herschel-Bulkley fluid to infinitesimal disturbances was studied for different values of n and Hb. Using normal-mode approach, i.e., the disturbance field is assumed of the form $\psi(r)\exp[i(\alpha z + m\theta - \omega t)]$, where α and m are respectively the axial and azimuthal wave numbers and ψ stands for pressure or any component of the disturbance velocity vector. The numerical results lead to the conclusion that the flow configuration $(0,\ 0,\ U_\ell(r))$ is linearly stable for all Reynolds numbers $Re = (\rho U_B D)/\mu_w$, where μ_w is the wall-shear viscosity. This result could be anticipated on the basis of [14], which however pertains to Bingham-type fluids.

When a small perturbation composed by a weighted combination of linear eigenfunctions is considered, there is a potential for a short-time amplification of the energy perturbation. This is a consequence of the non-normality of the linear stability operator, the eigenfunctions being not orthogonal under the energy norm. The transient evolution of the disturbance kinetic energy is determined following the same methodology as in [15]. For a given Fourier mode, the maximum amplification of the kinetic energy at any instant time is denoted G and the maximum of G for all pairs $(\alpha,\ m)$ is denoted G^{opt} and is reached by the optimal perturbation at a specific time t^{opt}. At the same dynamical and rheological parameters as in the experimental tests ($Re = 2420$, $n = 0.5$, $a = 0.1$), the numerical results show that the strongest linear transient growth is obtained for a travelling wave perturbation with $m = 2$ and $\alpha = 1.20$, giving $G^{opt} = 96.14$ reached after 8.98 time units R/U_B. The perturbation gains energy due to the inviscid Orr/lift-up mechanism. For comparison, in the case of streamwise independent perturbation with $m = 1$, we have $\sup_{t\geq 0} G \approx 31.9$. The cross-flow velocity vectors and the corresponding optimal streaks are represented in Fig. 1.

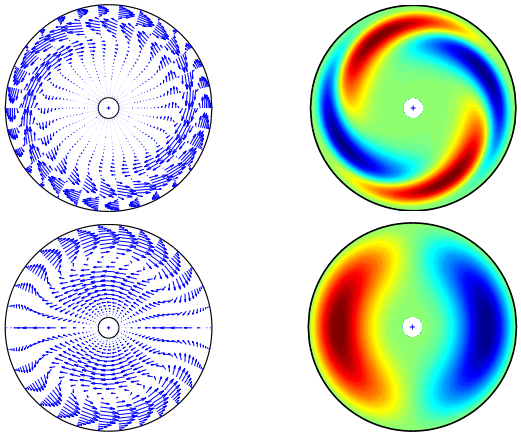

FIG. 1: Cross-flow in the $(r-\theta)$ section and optimal streaks at $Re = 2420$, $n = 0.5$ and $a = 0.1$. (Top): Optimal perturbation with $m = 2$ and $\alpha = 1.20$; (bottom) stream-wise independent vortices with $m = 1$. The red and blue zones correspond respectively to the fast and low streaks

Experimental setup. instrumentation and tested fluids. Full details of the flow facility and instrumentation have been given in [2] and so only a brief description is given here. Measurements were carried out in a plexiglass tube of internal diameter equal to 30 mm and 4.20 m long. This tube is longer than the entry length L_e necessary for the laminar flow to fully develop in all experiments carried out [16]. The velocity measurements were performed using a Dantec FlowLite system with a measuring volume 651 μm in length and 77 μm in diameter. The working fluid is a 0.2 w % aqueous solution of Carbopol 940. It is widely used as a model yield-stress fluid because of its stability and transparency. The rheological measurements were made with a controlled torque rheometer. It is found that for a large range of shear rates ($0.1\,\mathrm{s}^{-1} \leq \dot{\gamma} \leq 3\times 10^3\,\mathrm{s}^{-1}$), the flow curve is very well fitted by the Herschel-Bulkley model: $\tau = \tau_0 + K\dot{\gamma}^n$.

Results and discussion. A set of the measured mean axial velocity profiles at $z = 122\,D$ from the entrance section, in laminar, transitional and turbulent regimes is represented in Fig. 2(a). The measurements were done along a diameter in the horizontal median plane. As indicated above, the Reynolds number is defined with the wall shear-viscosity, calculated using the Herschel-Bulkley model fit at the wall shear-stress estimated from the pressure drop measurements. The continuous line is an average velocity profile $\bar{U}(r)$ obtained by taking the average of the velocity data from either side of the centreline. An indication on the flow regime is given by the near-wall $(r/R = 0.8)$ axial-velocity fluctuation level $u'(\mathrm{rms})/U_B$ vs Re displayed in Fig. 2(b). In the

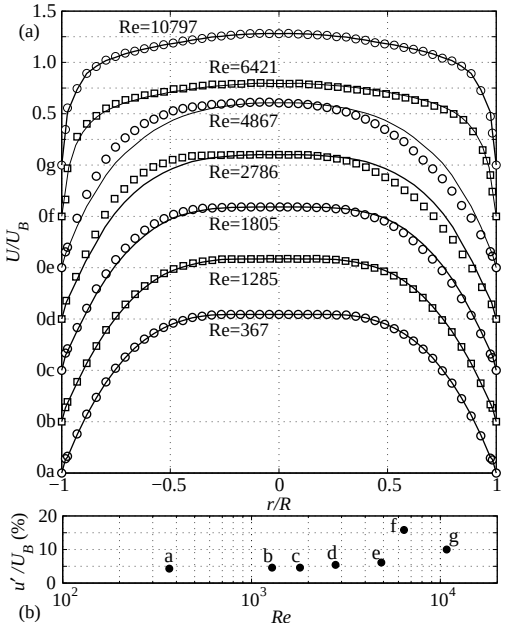

FIG. 2: (a) Mean axial velocity profiles at different Reynolds number, $\tau_0 = 9.75$ Pa, $K = 3.82$ Pa.s^n, $n = 0.47$; (b) Axial velocity fluctuations level $u'(rms)/U_B$ vs Re at $r/R = 0.8$.

laminar regime ($Re = 367$ and 1285) the axial velocity profiles are symmetric and in very good agreement with the theoretical profiles. In the transitional regime ($Re = 1805 - 4867$), an increasing asymmetry of the axial velocity profile with increasing Re is observed. The profiles $Re = 6421$ and $Re = 10797$ are symmetric, they correspond respectively to the end of transition (where (u'/U_B) is maximum) and turbulent flow.

In order to provide a three-dimensional description of the asymmetry observed in the transitional regime, axial velocity profiles were measured at three axial positions: $z = 20\,D$ (near the entrance section), $z = 54\,D$ (mid of the pipe) and $z = 122\,D$ and four azimuthal positions $\theta = 0$ (horizontal plan), $\pm\pi/4$ and $\theta = \pi/2$. The anti-clockwise orientation is adopted and the Reynolds number was fixed at $Re = 2420$. The obtained velocity profiles $U(r, \theta, z)$ are then written as the superposition of an average axial velocity profile $\bar{U}(r, z)$ and a streak $U_s(r, \theta, z)$. The azimuthal variation of U_s/U_B at different radial positions and at the three axial positions indicate clearly that $\frac{U_s(r,\theta,z)}{U_B}$ is well described by the relation: $\frac{U_s(r,\theta,z)}{U_B} = A(r, z)cos(\theta + \phi)$. As an example, Fig. 3 shows U_s/U_B vs θ at $r/R = 0.72$. The phase ϕ remains invariant along the pipe, and depends probably only on the inlet conditions. It is thus possible to draw the contours of iso-U_s in a cross section of the pipe, at each axial positions considered. The result of this procedure is given in Fig. 4. The red color (dark bottom) indicates regions where the flow of the fluid in the direction of the pipe is faster than the average profile, while the blue (dark top) denotes regions that are slower than

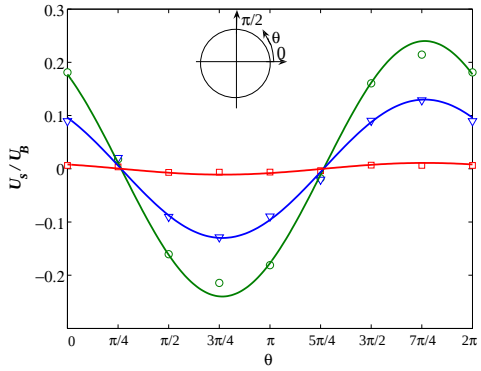

FIG. 3: Azimuthal variation of the streak velocity at $Re = 2420$, $r/R = 0.72$ and at the three axial positions: $z = 20\,D$ (square), $z = 54\,D$ (nabla) and $z = 122\,D$ (circle).

the average flow. These streaks suggest the existence of two counter-rotating longitudinal vortices, similar to those represented in Fig. 1 (bottom frames). Low shear

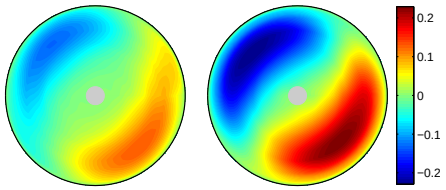

FIG. 4: Cross-section in (r, θ) at two axial positions $z/D = 54$ and 122 show contours of iso-$\left(U - \bar{U}\right)/U_B$, with the fast streaks (red/dark bottom) and low streaks (blue/dark top). $Re = 2420$, $n = 0.5$ and $a = 0.1$.

flow is advected from the wall towards the blue zone and large shear flow is advected towards the red zone. As in the case of the self-sustained cycle proposed by Waleffe [6], one can anticipate a shear flow instability of the streaks to regenerate the vortices. The visualization of this instability for instance from the velocity-time history signal displayed in Fig. 5 was not possible. Indeed, the frequency power spectra of the velocity fluctuations indicate that the dominant frequencies are practically less than 1 Hz without revealing any particular frequency. Therefore, this new coherent state is not a simple periodic travelling wave. It is worthy to note that there is a highly viscous central zone (larger than the theoretical plug zone) where u'/U_B remains at the same level as in laminar regime. With increasing Reynolds number, the diameter of this zone decreases to zero. In our experiments, u'/U_B on the axis starts to increase from $Re = Re_{c2} \approx 4000$ with the detection of turbulent spots, while the asymmetry is observed from $Re = Re_{c1} \approx 1800$. From $Re = Re_{c2}$, the flow cycles between the turbulent regime and the asymmetric state described above. The significance of the results described here is well analyzed in the framework of dynamical system theory. We can

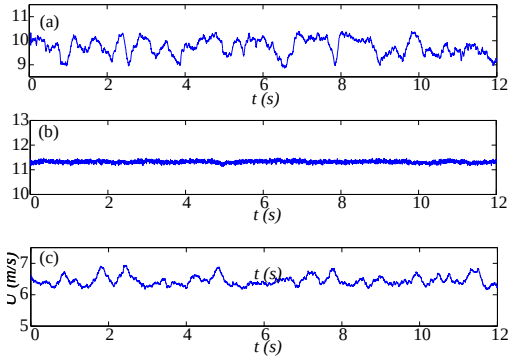

FIG. 5: Instantaneous axial velocity plots at $Re = 2420$, $z = 122\,D$, $n = 0.5$ and $r_0/R = 0.1$. (a) $r/R = 0.72$, $\theta = 7\pi/4$; (b) $r/R = 0$ and (c) $r/R = 0.72$, $\theta = 3\pi/4$.

choose to display them in a suitably defined phase subspace, such as that spanned by the rate of energy dissipation D per unit volume and the rate of energy input I per unit volume, along the lines of Biau *et al.* [17]. Steady states must fall on the line $I = D$ where the two quantities are in balance. In this subspace, the steady laminar flow is a linearly stable fixed point for all Re, and a global attractor for $Re < Re_{c1}$. In our case $Re_{c1} \approx 1800$, so that all initial conditions are attracted to the laminar node when $Re < Re_{c1}$. At $Re = Re_{c1}$, a new state, i.e., a stable non linear asymmetric state, is selected by the fluid. This new state may arise through a saddle-node bifurcation. Starting from $Re = Re_{c2} \approx 4000$, the basin of attraction of the asymmetric state decreases and point (2) in Fig. 6 ceases to be a global attractor; the flow trajectory can escape from the stable asymmetric node through a second saddle, follow this saddle's stable manifold and move towards point (3). After orbiting for a while around such a node (which represents the fully developed turbulent state) the flow can either be directed towards local attractor represented by node (2) or it can escape through yet another low-dimensional saddle towards a different region of phase space. The view just outlined, admittedly speculative, is supported by all available experimental results.

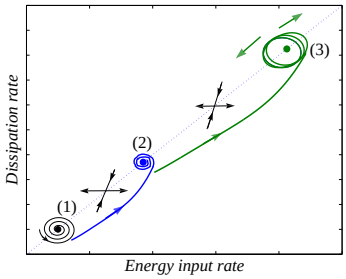

FIG. 6: Qualitative description of the transition process in the phase diagram displaying dissipation rate versus energy input rate. Point (1) is the steady, one-dimensional laminar state, towards which, the system returns spirally when $Re < Re_{c1}$. Point (2) is the non-linear stable asymmetric state. Node (3) represents the fully developed turbulent regime. The crosses with arrows sketch unstable saddle nodes. Flow trajectories are sketched for increasing values of Re.

Conclusion. The following conclusions can be drawn from this study: (1) Optimal disturbances are not useful to describe early stages of transition; (2) the non-linear asymmetric states observed are remarkably stable and persist for the whole duration of the experiments (several weeks); (3) such non-linear coherent states are qualitatively similar to the *edge-states* recently computed in the Newtonian case [3–5], although in the present context the vortices are closer to the wall because of presence of highly viscous fluid near the pipe axis; (4) stable asymmetric solutions act as local attractors in phase space. As Re is increased from zero, the basin of attraction of this asymmetric state increases, then it shrinks.

Acknowledgment. The authors are very grateful to Professors A. Bottaro and J.P. Brancher for fruitful discussions.

[1] M. P. Escudier and F. Presti, J. non-Newtonian Fluid Mech. **62**, 291 (1996).
[2] J. Peixinho, C. Nouar, C. Desaubry, and B. Théron, J. non-Newtonian Fluid Mech. **128**, 172 (2005).
[3] C. Pringle and R. Kerswell, Phys. Rev. Lett. **99**, 074502 (2007).
[4] T. Schneider, B. Eckhardt, and J. A. Yorke, Phys. Rev. Lett. **99**, 034502 (2007).
[5] B. Eckhardt, T. Schneider, B. Hof, and J. Westerweel, Annu. Rev. Fluid Mech. **39**, 447 (2007).
[6] F. Waleffe, Phys. Fluids **9**, 889 (1997).
[7] F. Waleffe, Phys. Rev. Lett. **81**, 4140 (1998).
[8] H. Faisst and B. Eckhardt, Phys. Rev. Lett. **91**, 224502 (2003).
[9] H. Wedin and R. R. Kerswell, J. Fluid. Mech. **508**, 333 (2004).
[10] B. Hof, C. V. Doorne, J. Westerweel, F. Nieuwstadt, H. Faisst, B. Eckhardt, H. Wedin, R. Kerswell, and F. Waleffe, Science. **305**, 1594 (2004).
[11] M. P. Escudier, R. J. Poole, F. Presti, C. Dales, C. Nouar, C. Desaubry, C. Graham, and L. Pullum, J. non-Newtonian Fluid Mech. **128**, 172 (2005).
[12] S. Eliahou, A. Tumin, and I. Wignanski, J. Fluid Mech. **361**, 333 (1998).
[13] M. Rudman, H. M. Bmackburn, L. J. W. Graham, and L. Pullum, J. non-Newtonian Fluid Mech. **1118**, 33 (2004).
[14] C. Nouar, N. Kabouya, J. Dusek, and M. Mamou, J.

Fluid. Mech. **577**, 211 (2007).
[15] P. J. Schmid and D. S. Henningson, *Stability and transition in shear flows* (Springer - Verlag, New York, 2001).
[16] G. B. Froishteter and G. V. Vinogradov, Rheol. Acta. **19**, 443 (1980).
[17] D. Biau, H. Soueid, and A. Bottaro, submitted to J. Fluid. Mech. (2007).